Normal, degenerated, and anomalous-dispersion-like Cerenkov sum-frequency generation in one nonlinear medium

Ning An,[1,2,3] Yuanlin Zheng,[1,3,5] Huaijin Ren,[4] Xiaohui Zhao,[1,3] Xuewei Deng,[4] and Xianfeng Chen[1,3,*]

[1]*Department of Physics and Astronomy, Shanghai Jiao Tong University, Shanghai 200240, China*
[2]*Shanghai Institute of Laser Plasma, Shanghai, China*
[3]*Key Laboratory for Laser Plasma (Ministry of Education), IFSA Collaborative Innovation Center, Shanghai Jiao Tong University, Shanghai 200240, China*
[4]*China Academy of Engineering Physics, Mianyang, Sichuan 621900, China*
[5]*e-mail: 5040729023@sjtu.edu.cn*
**Corresponding author: xfchen@sjtu.edu.cn*

Received January 15, 2015; revised March 21, 2015; accepted March 23, 2015; posted April 2, 2015 (Doc. ID 231669); published April 29, 2015

We report on the experimental realization of Cerenkov sum-frequency generation across the material dispersion in a one-dimensional, periodically poled ferroelectric crystal. Three schemes of sum-frequency generation, confined only in the vicinity of domain walls and in the form of nonlinear Cerenkov radiation, are demonstrated in normal, degenerated, and anomalous-dispersion-like configurations. We exploit their phase-matching geometries, which exhibit a whole scenario of the evolution of Cerenkov radiation varying with the dispersion relationship among the interaction waves. In addition, two sets of conical sum-frequency generation with different radius and center are demonstrated, which result from scattering assistant phase-matching processes.

OCIS codes: (190.7220) Upconversion; (190.0190) Nonlinear optics; (290.0290) Scattering.
http://dx.doi.org/10.1364/PRJ.3.000106

1. INTRODUCTION

Owing to the presence of the dispersion, the speed of moving charge particles in a dielectric medium may exceed that of light, which would drive the induced polarization to emit coherent electromagnetic waves in the form of Cerenkov radiation [1,2]. Characteristics in such processes contain the so-called velocity constraint, a forward-pointing conical wavefront and front-pointing energy propagation. The analogous phenomenon, nonlinear Cerenkov radiation (NCR), emerges in nonlinear optics when intense laser is injected into nonlinear media and gives rise to coherent harmonic generation in the Cerenkov direction [3,4]. The nonlinear Cerenkov angle is defined as $\cos\theta = \nu/\nu'$, where ν' and ν denote the phase velocity of the nonlinear polarization wave and harmonic wave, respectively. Phase matching of NCR is straightforward in normal dispersive nonlinear media. Previous studies [5,6] have revealed that the existence of domain walls in nonlinear ferroelectric crystals enhances the efficiency of NCR [7–10] and also modulates its behavior [11]. The process is accessible along domain walls even with moderate input light intensity. Since the nonlinear polarization wave only propagates (or is confined) along domain walls, its phase velocity could be determined as $\nu_p = \nu/\cos\gamma$, where γ is the angle between the plane of domain walls and the incident wave in the crystal. Based on this, researchers had proposed an anomalous-dispersion-like phase-matching scheme and approached particular nonlinear effects that were previously inaccessible under normal dispersion [11,12]. With proper incidence condition, it is possible to "accelerate" the phase velocity of nonlinear polarization and even break through the "prohibited threshold" of NCR in anomalous dispersion media. By exploiting the dispersion characteristics of polarization, highly efficient frequency doubling resulting from noncollinear phase-matching schemes on the surface [13] and boundary [14,15] of bulk anomalous crystals has been experimentally demonstrated which has great potential for practical applications.

Previous studies have mainly used second-harmonic generation schemes to detect and investigate such phenomena; for instance, the first observation of such enhancement by Fragemann in 2004 [5], NCR frequency conversion [16], the very latest 3D imaging of domain wall structures [8,17], and so on. In this work, we reveal a variety of NCR patterns that occur in a single photonic crystal under different dispersion circumstances. By varying the wavelengths of two collinear incident waves, we observe a series of consecutively evolving upconversion processes which manifest themselves as normal, degenerated, and anomalous-dispersion-like NCR type sum-frequency generation (SFG). In addition, multiconical SFG has been observed which results from two types of scattering-assistant phase-matching geometries.

2. EXPERIMENTAL SETUP

To demonstrate the Cerenkov-type SFG scenarios, two collinear laser beams with frequencies ω_1 and ω_2 are mildly focused into a nonlinear photonic crystal, as shown in the experimental layout in Fig. 1(a). The light source is an optical parametric amplifier (OPA, TOPAS, Coherent Inc.) pumped

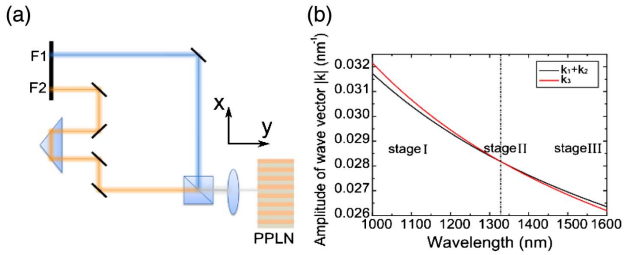

Fig. 1. (a) Layout of experimental setup. $\lambda_1 = 800$ nm, $\lambda_2 = 1000$ nm–1600 nm. (b) Theoretical curves of the wave vector relationship of the interaction wave beams, where the incidences are both set to be ordinary polarized and the SFG extraordinary polarized.

by a Ti:Sapphire femtosecond regenerative amplifier system (50 fs duration, 1 kHz rep. rate). Two wave beams from the OPA, the residual pump (F1) centered at 800 nm and the signal (F2), tunable from 1000 to 1600 nm (both ordinarily polarized), are synchronized and loosely focused into the sample along the y axis. The sample used in the experiment is a periodically poled 5 mol.% MgO:$LiNbO_3$ crystal with dimensions of 15 mm(x) × 5 mm(y) × 0.5 mm(z) and period of 30 μm. The incident beams are collimated and propagated along the domain walls of the sample.

3. EXPERIMENTAL RESULTS AND ANALYSIS

The role of dispersion underlying the fundamental waves and SFG varying with incident wavelength under the oo-e phase-matching condition is shown in Fig. 1(b). There are three cases of the wave vector relationship among the interaction beams: I. $k_1 + k_2 < k_3$, II. $k_1 + k_2 = k_3$, and III. $k_1 + k_2 > k_3$. Case I shows the normal dispersion circumstance where the Cerenkov SFG condition is naturally satisfied. Normal sum-frequency NCR could be expected. In case II, the nonlinear Cerenkov degenerates into a forward-pointing wavefront, and thus the wave vectors of fundamental and harmonic waves are parallel to each other. As regards case III, since the phase velocity of sum-frequency nonlinear polarization does not exceed that of the harmonic wave, this would result in no NCR generation in the normal incidence configuration. However, when the fundamental waves propagate with anangle of γ with respect to the domain wall, the phase velocity of the sum-frequency nonlinear polarization can be expressed as

$$v_p = \frac{\omega_3}{\left(\frac{\omega_1}{v_1} + \frac{\omega_2}{v_2}\right)\cos\gamma}, \tag{1}$$

where ω_3 denotes the sum frequency and v_1, v_2 are the phase velocities of waves F1 and F2, respectively. In this case, by adjusting the incident angle, the phase velocity of sum-frequency nonlinear polarization could be accelerated and even exceeds that of the harmonic in the anomalous dispersion environment, finally resulting in nonlinear Cerenkov SFG. The modulated Cerenkov SFG angle with respect to domain wall is expressed as

$$\cos\theta = \frac{(|\vec{k}_1| + |\vec{k}_2|)\cos\gamma}{|\vec{k}_3|}, \tag{2}$$

where k_1, k_2, and k_3 are the wave vectors of the fundamental waves and harmonic wave, respectively.

In our experiment, typical recorded patterns of the predicated three cases, with the wavelength of F2 tuned across the range of 1000–1600 nm, are demonstrated in Figs. 2(a), 2(b), and 2(c), respectively. For the first case, Cerenkov SFG generation and Cerenkov second-harmonic generation (CSHG) are displayed with fundamental waves (F1/F2) centered at 800/1250 nm, while the phase-matching condition is illustrated in Fig. 2(d). The outer pair of harmonic spots is the Cerenkov frequency doubling of incident wave F1, whose central wavelength is 400 nm and the external angle is 33.1°. The inner pair of harmonic spots is the Cerenkov SFG of F1 and F2. It is noted that the refractive index of the o-polarized fundamental F2 exceeds the e-polarized harmonic at the input wavelength range, which actually mimics an anomalous dispersion environment in the oo-e phase-matching geometry. In this case, a conical scattering-assistance second-harmonic beam emerged instead of NCR, which is in accordance with our previous studies [18].

When the incident wavelengths reach case II, the momentum conservation law between the fundamental waves and generated harmonic waves is fulfilled in the collinear arrangement [see Fig. 2(e)]. The collinear phase matching between fundamental and sum-frequency waves is thus fulfilled, which would maximize the conversion efficiency. This circumstance is distinguished from the collimated SFG in bulk media in that the confinement effect of domain walls greatly enhances the nonlinear polarization and improves the sum-frequency intensity. Thus, the enhancement is only localized to their vicinity regions. The measured conversion efficiency is up to 10.2%, which will be of value for efficient frequency conversion technology and other optical applications. In this way, the degenerated NCR shows similarities and differences of essential physical features with common collinear $\chi^{(2)}$ upconversion processes, which deserves further investigation.

In case III, there is no NCR generation in the normal incidence configuration, which is in agreement with our theoretical predication. By rotating the incident angle, the NCR can even exist in such anomalously dispersive media while the modulated Cerenkov condition [Eq. (2)] is satisfied. Figure 2(f) illustrates the phase-matching geometry in such a configuration, where the pair of harmonic spots appears on the same side of incidence. Overall, a successive scheme of normal, degenerated, and anomalous-dispersion-like Cerenkov SFG can be realized in one nonlinear crystal.

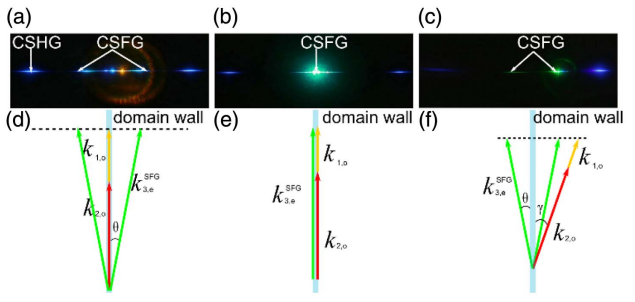

Fig. 2. (a)–(c) Illustrations of the typical patterns with the wavelength of incidence F2 at 1250 nm, 1340 nm, and 1450 nm, respectively. (d)–(f) Schematics of the phase-match conditions of the Cerenkov sum-frequency generation (CSFG) in normal dispersion, degenerated, and anomalous dispersion stage, respectively.

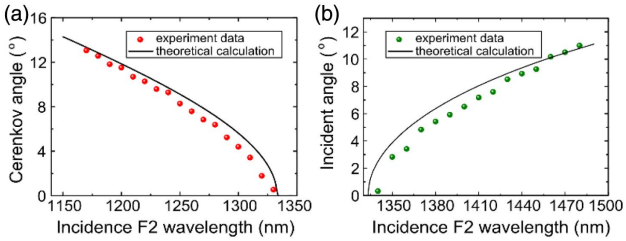

Fig. 3. (a) Experimental data (red spots) and simulation (solid line) of the external angle of the Cerenkov generation as a function of incident wavelength. (b) Experimental data (green spots) and simulation (solid line) of the incident angle at degenerated stage as a function of incident wavelength.

The unified external angles of the Cerenkov SFG depend on the fundamental wavelengths and incident angles throughout all types of the dispersion condition. For normal pump incidences, we measured the external angle θ of the Cerenkov SFG varying with the incident wavelength, as shown in Fig. 3(a). The dependence exhibits monotonically decrease with the increasing wavelength of the incidences until the degenerated circumstance. Beyond this point, Cerenkov generation can still be obtained by rotating the incident angle to satisfy Eq. (2) in such an anomalously dispersive medium. For simplicity, we studied the critical situation while varying the incident angle to generate the degenerated Cerenkov SFG. Corresponding to $\theta = 0°$, the measured incident angle varying with input wavelength is shown in Fig. 3(b), which agrees well with the prediction.

Additionally, in the third case, two sets of multiple conical second-harmonic generations were observed in the normal incident circumstance, which share the same wavelength but different central locations [see Fig. 4(a)]. Owing to the random refractive-index inhomogeneity and imperfection inside the crystal [19,20], each incident beam experiences scattering, with scattered light exhibiting a consecutively and symmetrically spatial distribution. These two series of multiple rings originate from the scattering-assistant SFG. Geometries for these conical SFGs at normal incidence are schematically illustrated in Figs. 4(b) and 4(c). The phase-matching conditions for the conical SFG emissions are expressed as

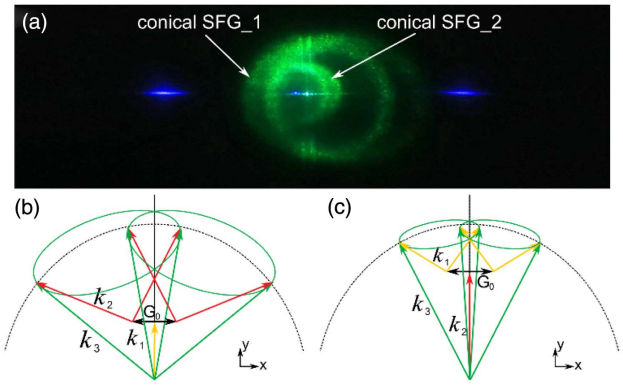

Fig. 4. (a) Experimental pattern of the two sets of multiple conical harmonic generations. (b), (c) Phase-matching geometries for conical SFG 1 and conical SFG 2, respectively. Each incidence mixes with the scattered lights of the other incidence, giving birth to multiple scattering rings with different radii and center locations.

$$\vec{k}_1 + \vec{k}_2' + m\vec{G}_0 = \vec{k}_3, \vec{k}_2 + \vec{k}_1' + m\vec{G}_0 = \vec{k}_3, \qquad m = 1, 2\ldots, \tag{3}$$

where $\vec{k}_1'$, $\vec{k}_2'$ represent the scattering wave vectors of the incident waves. The intensity of the scattering conical SFG can be expressed as $I_3^1 \propto I_1 I_2' L^2$, $I_3^2 \propto I_2 I_1' L^2$ where L is the interaction length and I_1, I_2, I_1', I_2' are the intensity of incidences and the corresponding scattering light, respectively. The radii of the rings increase synchronously with the increment of incident wavelengths. Considering that the conical ring pattern contains the structure information of the $\chi^{(2)}$ crystal, such a scattering recording mechanism may have great potential in nondestructive evaluation of ferroelectric domain structures [20,21] and other applications.

4. CONCLUSION

In conclusion, a generic successive picture of Cerenkov SFG, from normally dispersive to anomalously dispersive schemes, has been realized in one nonlinear crystal. Analysis of the three stages indicates that the Cerenkov phase-matching geometries vary with the dispersion condition. It is noteworthy that the degenerated Cerenkov generation localized in the domain wall region is achieved with a forward-pointing wavefront, which is in coincidence with the collinear harmonic generation process. The Cerenkov external angle dependence on the input wavelengths is investigated experimentally and agrees well with the prediction. Moreover, two sets of multiple conical harmonic generations are demonstrated under anomalous dispersion, resulting from the sum frequency by the scattering phase-matching processes of each incidence.

REFERENCES

1. P. A. Cherenkov, "Visible emission of clean liquids by action of γ radiation," Doklady Akademii Nauk SSSR **2**, 451 (1934).
2. C. Luo, M. Ibanescu, S. G. Johnson, and J. Joannopoulos, "Cerenkov radiation in photonic crystals," Science **299**, 368–371 (2003).
3. Y. Zhang, Z. Gao, Z. Qi, S. Zhu, and N. Ming, "Nonlinear Čerenkov radiation in nonlinear photonic crystal waveguides," Phys. Rev. Lett. **100**, 163904 (2008).
4. C. Ma, Y. Wang, L. Liu, X. Fan, A. Qi, Z. Feng, F. Yang, Q. Peng, Z. Xu, and W. Zheng, "Dark blue Cerenkov second harmonic generation in the two-layer-stacked hexagonal periodically poled MgO:$LiNbO_3$s," Chin. Opt. Lett. **12**, 030501 (2014).
5. A. Fragemann, V. Pasiskevicius, and F. Laurell, "Second-order nonlinearities in the domain walls of periodically poled $KTiOPO_4$," Appl. Phys. Lett. **85**, 375–377 (2004).
6. X. Deng and X. Chen, "Domain wall characterization in ferroelectrics by using localized nonlinearities," Opt. Express **18**, 15597–15602 (2010).
7. K. Kalinowski, P. Roedig, Y. Sheng, M. Ayoub, J. Imbrock, C. Denz, and W. Krolikowski, "Enhanced Čerenkov second-harmonic emission in nonlinear photonic structures," Opt. Lett. **37**, 1832–1834 (2012).
8. Y. Zhang, F. Wang, K. Geren, S. Zhu, and M. Xiao, "Second-harmonic imaging from a modulated domain structure," Opt. Lett. **35**, 178–180 (2010).
9. H. Huang, C.-P. Huang, C. Zhang, D. Zhu, X.-H. Hong, J. Lu, J. Jiang, Q.-J. Wang, and Y.-Y. Zhu, "Second-harmonic generation in a periodically poled congruent $LiTaO_3$ sample with phase-tuned nonlinear Cherenkov radiation," Appl. Phys. Lett. **100**, 022905 (2012).
10. K. Kalinowski, Q. Kong, V. Roppo, A. Arie, Y. Sheng, and W. Krolikowski, "Wavelength and position tuning of Cerenkov second-harmonic generation in optical superlattice," Appl. Phys. Lett. **99**, 181128 (2011).

11. H. Ren, X. Deng, Y. Zheng, N. An, and X. Chen, "Nonlinear Cherenkov radiation in an anomalous dispersive medium," Phys. Rev. Lett. **108**, 223901 (2012).
12. X. Zhao, Y. Zheng, H. Ren, N. An, and X. Chen, "Cherenkov second-harmonic Talbot effect in one-dimension nonlinear photonic crystal," Opt. Lett. **39**, 5885–5887 (2014).
13. H. Ren, X. Deng, Y. Zheng, N. An, and X. Chen, "Surface phase-matched harmonic enhancement in a bulk anomalous dispersion medium," Appl. Phys. Lett. **103**, 021110 (2013).
14. H. Ren, X. Deng, Y. Zheng, N. An, and X. Chen, "Enhanced nonlinear Cherenkov radiation on the crystal boundary," Opt. Lett. **38**, 1993–1995 (2013).
15. X. Wang, H. Ren, N. An, X. Zhao, Y. Zheng, and X. Chen, "Large acceptance of non-collinear phase-matching second harmonic generation on the surface of an anomalous-like bulk dispersion medium," Opt. Express **22**, 28234–28239 (2014).
16. Y. Sheng, S. M. Saltiel, W. Krolikowski, A. Arie, K. Koynov, and Y. S. Kivshar, "Čerenkov-type second-harmonic generation with fundamental beams of different polarizations," Opt. Lett. **35**, 1317–1319 (2010).
17. Y. Sheng, A. Best, H.-J. Butt, W. Krolikowski, A. Arie, and K. Koynov, "Three-dimensional ferroelectric domain visualization by Čerenkov-type second harmonic generation," Opt. Express **18**, 16539–16545 (2010).
18. N. An, Y. Zheng, H. Ren, X. Deng, and X. Chen, "Conical second harmonic generation in one-dimension nonlinear photonic crystal," Appl. Phys. Lett. **102**, 201112 (2013).
19. Y. Ja, "A scattered ring in a natural crystal of tourmaline," J. Opt. **21**, 41 (1990).
20. K. Bastwöste, U. Sander, and M. Imlau, "Conical light scattering in strontium barium niobate crystals related to an intrinsic composition inhomogeneity," J. Phys. Condens. Matter **19**, 156225 (2007).
21. P. Xu, S. Ji, S. Zhu, X. Yu, J. Sun, H. Wang, J. He, Y. Zhu, and N. Ming, "Conical second harmonic generation in a two-dimensional $\chi^{(2)}$ photonic crystal: a hexagonally poled $LiTaO_3$ crystal," Phys. Rev. Lett. **93**, 133904 (2004).